Chemistry–A European Journal
Research Article
doi.org/10.1002/chem.202301795
Chemistry Europe
European Chemical Societies Publishing
www.chemeurj.org

DFT Study of Imine-Exchange Reactions in Iron(II)-Coordinated Pincers

Annemieke van Dam,[a] Robin van Schendel,[a] Satesh Gangarapu,[a] Han Zuilhof,*[a, b] and Maarten M. J. Smulders*[a]

The imine bond is among the most applied motifs in dynamic covalent chemistry. Although its uses are varied and often involve coordination to a transition metal for stability, mechanistic studies on imine exchange reactions so far have not included metal coordination. Herein, we investigated the condensation and transimination reactions of an Fe^{2+}-coordinated diimine pyridine pincer, employing wB97XD/6-311G(2d,2p) DFT calculations in acetonitrile. We first experimentally confirmed that Fe^{2+} is strongly coordinated by these pincers, and is thus a justified model ion. When considering a four-membered ring-shaped transition state for proton transfers, the required activation energies for condensation and transimination reaction exceeded the values expected for reactions known to be spontaneous at room temperature. The nature of the incoming and exiting amines and the substituents on the *para*-position of the pincer had no effect on this. Replacing Fe^{2+} with Zn^{2+} or removing it altogether did not reduce it either. However, the addition of two ethylamine molecules lowered the energy barriers to be compatible with experiment (19.4 and 23.2 kcal/mol for condensation and transimination, respectively). Lastly, the energy barrier of condensation of a non-coordinated pincer was significantly higher than found for Fe^{2+}-coordinating pincers, underlining the catalyzing effect of metal coordination on imine exchange reactions.

Introduction

Since the start of the twenty-first century, dynamic covalent chemistry has become increasingly popular.[1] The characteristic combination of reversibility and robustness that defines dynamic covalent bonds has enabled a variety of new concepts and applications in various fields, ranging from dynamic combinatorial libraries to supramolecular chemistry and from molecular machines to materials chemistry.[2–8] For example, in the field of polymer chemistry, covalent adaptable networks (CANs)[9–11] have shown to be a new class of polymers with the robustness of thermosets but the malleability and repairability of thermoplasts,[12–14] bringing degradability and recyclability of network polymers within reach.[15] In the field of supramolecular chemistry, the use of dynamic covalent chemistry has led to the formation of self-assembled cages, largely driven by the possibility of a thermodynamically controlled assembly of large complexes.[16–20] These cages can be used for the transport of small chemicals,[21] but also allow reactions to take place in an artificially high concentration in its confined space.[22] Furthermore, the operation of molecular walkers[23] and the synthesis of metal–organic frameworks[24] hinge on dynamic covalent chemistry.

The dynamic covalent bond motif that is among the most explored is the imine bond, or Schiff base.[25] This imine bond can undergo various dynamic reactions,[26] none of which require a metal catalyst.[27] Imine exchanges have been used in molecular machines, where an aldehyde can 'walk' along a chain of amines.[28] In cages, the imine bond is also vastly popular, as the bond's dynamic nature allows for error-checking during the assembly of the – typically – large number of components that need to come together in a single cage structure.[18,29–30] Also, within the context of systems chemistry, the imine bond has been used to establish dynamic combinatorial libraries that can collapse upon addition of a suitable target/template.[31–34] Finally, for covalent organic frameworks,[35–38] the dynamic imine bond is crucial to their (equilibrium) synthesis and for their ultimate structure and performance.

Imines are formed reversibly from an aldehyde and an amine. Due to the large variation in commercially available aldehydes and amines, the imine motif offers ample opportunity to create a macrostructure with the desired function or properties. Moreover, exchange of material-bound amines,[39] for example from an alkylamine or hydrazine to an alkoxyamine, offers the possibility to – post-synthetically – alter a functionality of a material.

[a] A. van Dam, R. van Schendel, Dr. S. Gangarapu, Prof. H. Zuilhof, Dr. M. M. J. Smulders
Laboratory of Organic Chemistry
Wageningen University
Stippeneng 4, 6708WE Wageningen (The Netherlands)
E-mail: han.zuilhof@wur.nl
maarten.smulders@wur.nl

[b] Prof. H. Zuilhof
School of Pharmaceutical Sciences and Technology
Tianjin University
92 Weijin Road, Tianjin 300072 (P.R. China)

Supporting information for this article is available on the WWW under https://doi.org/10.1002/chem.202301795

A general drawback of imines for materials science is their tendency to hydrolyze.[40] Coordination to a transition metal has been shown to drastically reduce this effect,[41] without hindering the responsive character of the structure. Imine-metal complexes can form stable structures, displaying two orthogonal types of changeability: both the C=N imine bond and the N–M coordination bond can undergo reversible reactions. This so-called "subcomponent self-assembly" has been showcased first by Nitschke and Lehn,[42] and has since then been widely applied in metal–organic cage syntheses.[21,43–46] Not only cages, but also other types of structures such as grids,[47] macrocycles[48] and metallogels,[49] can be formed by subcomponent self-assembly.[50–51]

Our group has taken the double versatility of imine-metal coordination complexes and applied it to polymeric systems.[52] We created a 2,6-diimine pyridine pincer motif that is connected via a linker to another identical pincer motif. This was shown to create networks with physical properties that could be altered by external stimuli, both via imine exchange reactions and through replacement of the metal center. These networks have been developed in organic solvents, such as acetonitrile. Furthermore, this traditional 2,6-diimine pyridine pincer motif[53] has also been used in cages,[54] knots,[55] tunable gas membranes[56] and other (self-healing) polymer networks.[57–59] While in our previous work, we mostly considered Zn^{2+} for the construction of dynamic coordination polymers,[52] the 2,6-diimine pyridine pincer motif has been combined with a large number of transition metals, including Mn^{2+}, Fe^{2+}, Co^{2+}, Ni^{2+}, Cu^{2+}, Zn^{2+}, Cd^{2+}, Hg^{2+}, and Pd^{2+}.[60–62]

In contrast to the wide range of applications that rely on imine bonds and imine bond exchange reactions, the full mechanistic details of the underlying exchange reactions of imine pincers have received very little attention. It is well-known that Schiff bases can undergo three imine exchange reactions: condensation, with hydrolysis as its reverse reaction, transimination and imine metathesis (Scheme 1).[27] In condensation, the amine attacks the aldehyde to first form a carbinolamine, followed by elimination of water. Transimination is the attack of an amine group on the carbon of the imine, creating an aminal, after which the original amine leaves, and the attacking amine forms an imine bond with the carbon. In imine metathesis, two imine moieties find each other, and through a double [2,2]-metathesis, the carbon and nitrogen atoms of the imines switch partners.

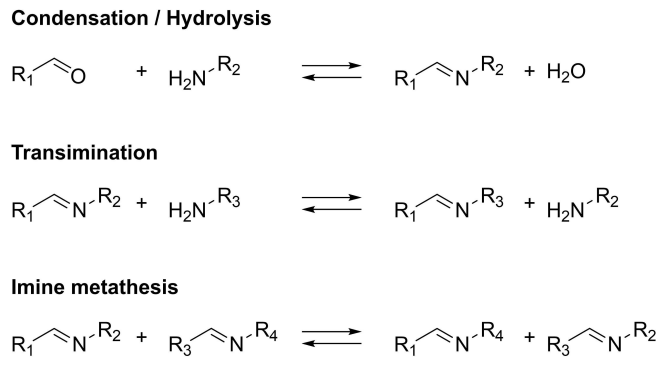

Scheme 1. Three reversible reactions of Schiff bases: condensation, with hydrolysis as the reverse reaction, transimination and imine metathesis.

Over the years, insightful computational research has been done on imine exchange reactions.[27] Ciaccia and co-workers have calculated the transimination and condensation reactions in the presence of primary amines.[63] They suggested a four-membered ring transition state for the proton transfers to be the most likely pathway, as opposed to consecutive protonation and deprotonation. If water is present, the energy of the proton transfer transition states can be lowered by using one or two water molecules as proton shuttles, forming a six- or eight-membered ring, respectively.[64–65] Primary amines can also take up this role, but their effect is less than that of water. Zheng and co-workers have shown that non-covalent interactions of an electron donor with an imine or aldehyde can significantly reduce imine exchange rates.[66] In their case, the interaction was a hydrogen bond. To the best of our knowledge, and in contrast to the rapidly rising amount of experimental work that has been reported,[21,67–68] the effect of coordination with transition metals on imine exchanges has not yet been studied theoretically, even though it is known that metal coordination alters the electronic and structural shape of a ligand.[69]

In this work, we explore the imine exchange reactions of Fe^{2+}-pincer complexes in acetonitrile by computational means. Using a state-of-the-art functional and basis set (wB97XD/6-311G(2d,2p)) for our DFT calculations, we investigate the condensation and transimination reactions of a range of pincers. Various amines and imines are considered, and the effect of the pyridine *para*-position's nucleophilicity is included (Figure 1). For the final proton transfer from carbinolamine and aminal species to the separate products, both a previously proposed four-membered transition state[63] and two ethylamines as proton shuttles are considered. As pincers drastically reduce the freedom of movement of individual imine moieties, imine metathesis is considered unlikely and therefore not part of the investigation.

Results and Discussion

Following our previous report on the use of Zn^{2+} as metal ion to coordinate to a 2,6-diimine pyridine ligand,[52] our current aim was first to see whether a stronger binding metal ion would be available. Following literature on the use of Fe^{2+} as alternative metal ion in polymeric systems featuring a similar

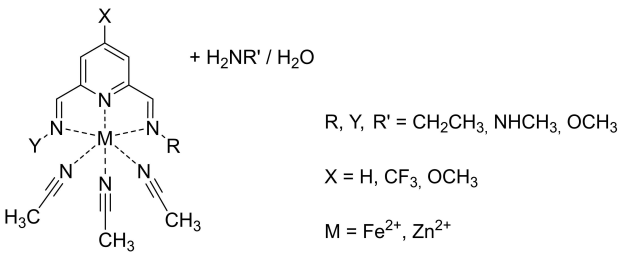

Figure 1. Imine pincer complexes under current study that are formed via condensation or transimination.

pincer motif,[56] and keeping the availability of this innocuous metal in mind, we set out to determine whether our 2,6-diimine pyridine ligand would indeed bind more strongly to Fe^{2+}. As the complexation of the metal ion to the ligand leads to strong coloration of the solution (Figure 2A), we performed a UV-vis titration to monitor formation of the metal-ligand complex (details in Supporting Information, section S1). We plotted the increase in absorption (at 370 nm for Zn^{2+} and at 613 nm for Fe^{2+}) as function of the equivalence of metal ion added (Figure 2B). Comparing the results for Zn^{2+} and Fe^{2+} in Figure 2B, it can be seen that, while both metal ions can bind strongly to the pincer, the binding for Fe^{2+} is strongest, as is evidenced by the steeper increase in absorption as function of equivalence of metal ion added, and by the fact that the maximum absorption is reached at lower equivalence of metal for Fe^{2+} than for Zn^{2+}. Our observations are in agreement with earlier work on structurally similar (tridentate) terpyridine-based ligands that also report a higher binding constant for binding

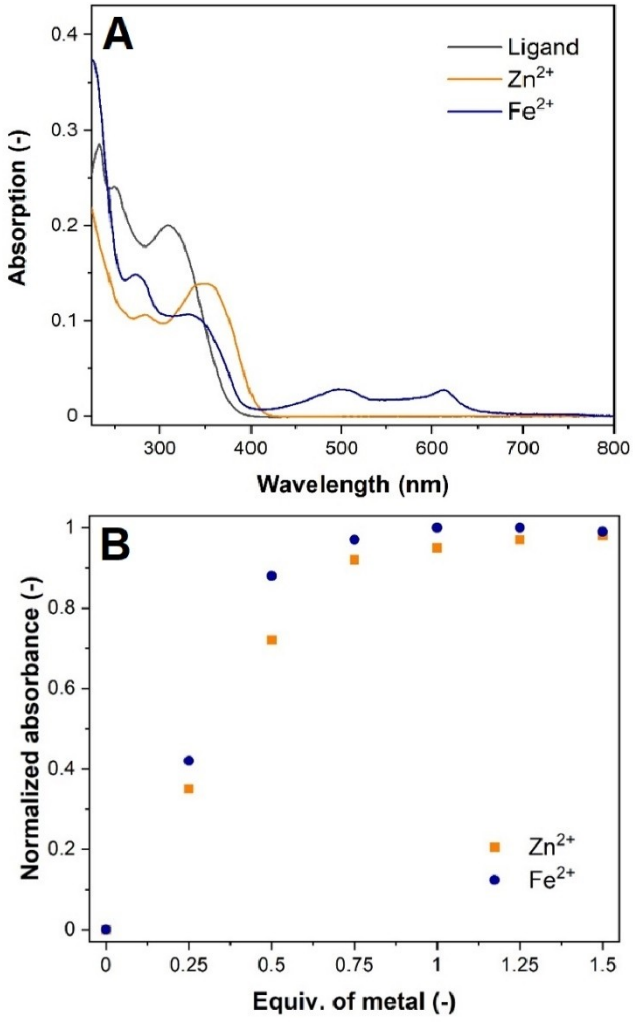

Figure 2. (A) UV-vis spectrum of the diiminepyridine ligand, and the diiminepyridine/metal complex (5 equiv of metal ion). Ligand concentration: $1.0 \cdot 10^{-5}$ M in acetonitrile. Path length: 1.0 cm. (B) Metal titration of Zn^{2+} or Fe^{2+} to the diiminepyridine ligand: the normalized absorption (recorded at 613 nm for Fe^{2+} and at 370 nm at Zn^{2+}) was plotted as a function of the equivalence of metal. Ligand concentration: $1.0 \cdot 10^{-5}$ M in acetonitrile.

to Fe^{2+} than to Zn^{2+}.[70] Given the stronger binding for Fe^{2+} we decided to focus our calculations on this metal ion, and only study the Zn^{2+} ion for specific cases.

Condensation Reaction Without Proton Shuttles

The condensation reaction between [iron(II) 2-methoxo-6-ethylimine pyridine $(NCCH_3)_3]^{2+}$ and ethylamine (Figure 3) initially yields a zwitterionic hemiaminal (**B**) at $\Delta G = -6.5$ kcal/mol driving force. In line with previous research,[27] a four-membered ring was taken as the transition state for the proton transfer from the nitrogen to the oxygen, at $\Delta G^{\ddagger} = 11.4$ kcal/mol (**TS-1**). The resulting hemiaminal (**C**) was found at $\Delta G = -8.8$ kcal/mol. Dihedral rotation from the hemiaminal with alcohol coordination to the one with amine coordination occurred via a transition state of $\Delta G^{\ddagger} = 3.0$ kcal/mol (**TS-2**). In this transition state, the bond length of Fe–O was significantly elongated from 2.07 Å to 3.00 Å, while the coordination of the amine did not yet start: the bond length is 3.39 Å in the transition state and only 2.08 Å in the resulting hemiaminal (**D**). Due to this dissociation, the energy barrier was higher than expected for a simple rotation. The hemiaminal with amine coordinated to the iron center (**D**) was at $\Delta G = -17.6$ kcal/mol significantly more stable than the hemiaminal with alcohol coordination (**C**). The second proton transfer was not followed by another zwitterionic intermediate, but immediately resulted in water elimination. The four-membered ring transition state (**TS-3**) was found with a relative Gibbs free energy of +34.0 kcal/mol, making this the rate-limiting step with a barrier of $\Delta G^{\ddagger} = 51.6$ kcal/mol. In this four-membered ring, the N–H bond at 1.46 Å and the O–H bond at 1.14 Å were at a strained 118.8°. This means no hydrogen bonding takes place in this transition state, explaining the extremely high energy barrier. The final compound (**E**) was found at $\Delta G = -16.7$ kcal/mol. However, due to the energy barrier of 51.6 kcal/mol, the condensation reaction via this pathway can be ruled out at room temperature in acetonitrile.

To investigate the effect of the metal center, this condensation reaction was also calculated without a metal and with Zn^{2+} as metal (Figure 3, in red and blue, respectively). Already in the first step the stabilizing role of the metal becomes very clear, with, for example, about a 10 kcal/mol difference of the metal-free system compared to the Fe^{2+}-stabilized complex. In addition, for the metal-free system the first proton transfer, yielding **TS-1**, now required 32.0 kcal/mol instead of 17.9 kcal/mol, while the barrier for the second proton transfer **TS-3** was not reduced significantly. In absence of a metal center, there is no rotation of the incoming nitrogen towards the metal center (i.e., **TS-2** does not exist and **D** is equal to **C**). Lastly, the driving force for the overall reaction from aldehyde to imine in the non-coordinated reaction is small, only 3.0 kcal/mol. Thus, without a metal, the barriers are not reduced but the driving force is largely lost.

As experimental work has been conducted with Zn^{2+} as well as Fe^{2+}, we also calculated the condensation reaction with Zn^{2+} as metal center (Figure 3, in blue). Adduct **B** formation gained less energy than with Fe^{2+} and the total energy gain is

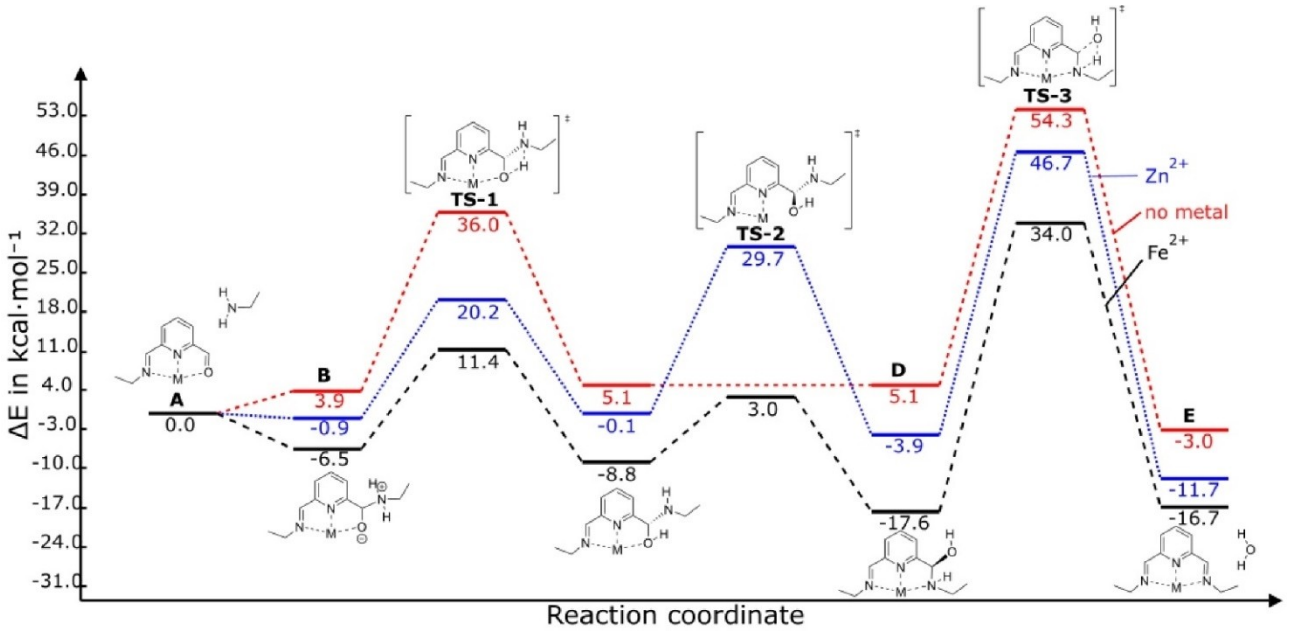

Figure 3. Gibbs free energy profile for the condensation reaction between ethylamine and [iron(II) 2-methoxo-6-ethylimine pyridine $(NCCH_3)_3]^{2+}$ (black), [zinc(II) 2-methoxo-6-ethylimine pyridine $(NCCH_3)_3]^{2+}$ (blue), and 2-methoxo-6-ethylimine pyridine (red), calculated without explicit solvation. All energy profiles are produced using free software from Angnes.[71] The second proton transfer, from **D** to **TS-3**, is rate-limiting in all cases with an energy barrier of 51.6, 50.6 and 49.2 kcal/mol, respectively. Note: For both the Fe^{2+} and Zn^{2+}-complex, even an extensive variation in computational parameters did not yield an activation energy of rotation (i.e., structure **TS-2** could not be localized). The maximum energy of the reaction coordinate scan (step size C–C bond torsion of 1°) was taken instead.

slightly less, both in line with our experimental findings that Fe^{2+} is stronger binding than Zn^{2+}. Proton transfers **TS-1** and **TS-3** have similar energy cost as with Fe^{2+}. However, the rotation **TS-2** required significantly more energy. This higher $\Delta G^{\ddagger}$ for rotation can be explained by the non-symmetrical octahedral coordination geometry that Zn^{2+} has formed, in which the three acetonitrile ligands are slightly pushed towards the non-reactive amine of the pincer, resulting in stronger binding of the reacting amine. In all, we can conclude that the condensation reaction is most favorable with Fe^{2+}, but also that a different pathway for proton transfer must be found.

It is known that the choice of functional in DFT can have an effect on the energy barriers that are found. To exclude this bias, we recalculated the Gibbs Free energies with B97D and MO6-2X of structures **A**, **D**, **TS-3** and **E** for the condensation reactions with Fe^{2+}, Zn^{2+} and without metal (Supporting Information S2). The condensation reactions were not more likely with these functionals, ruling out any method bias.

The final compound (**E**) was found at $\Delta G = -16.7$ kcal/mol. This value is expected to become more negative (i.e., approximately −22 to −23 kcal/mol) with improved explicit solvation of the released water, which is known to be insufficiently treated using implicit solvent models. Such additional explicit solvation (also relevant for the data in Figures 4–6) was demonstrated for release of water in the imine formation (Supporting Information S3), but this larger size due to additional freely 'floating' solvent molecules becomes, however, impractical – especially for the transition state calculations – while it is expected to only play a significant role when water is freely solvable, i.e., after release from the C atom. Therefore, we did not include it in the structures used to construct Figures 3–6, but note that with such additional solvation the imines become the most stable systems, as also found experimentally. However, although thus being thermodynamically attractive, due to the energy barrier of 51.6 kcal/mol, the condensation reaction via this pathway can be ruled out at room temperature in acetonitrile.

Transimination Reaction Without Proton Shuttles

Next to the imine formation (condensation) reaction, we also studied the imine exchange reaction by transimination, in which a free amine attacks an existing imine. Figure 4 (in black) shows the energy profile of the transimination reaction between [iron(II) 2,6-bis-ethylimine pyridine $(NCCH_3)_3]^{2+}$ and ethylamine, and (in red) the metal-free system. Both symmetric energy profiles with the four-membered ring transition state of the proton transfer yield activation energies of >34 kcal/mol. However, exchanges of imines, hydrazones and oximes occur readily at ambient conditions in acetonitrile. Oximes are more inert in neutral or basic conditions, yet become dynamic in acidic conditions.[72–73] Thus, the four-membered ring TS should be discarded as viable hypothesis, and other mechanistic routes need to be investigated.

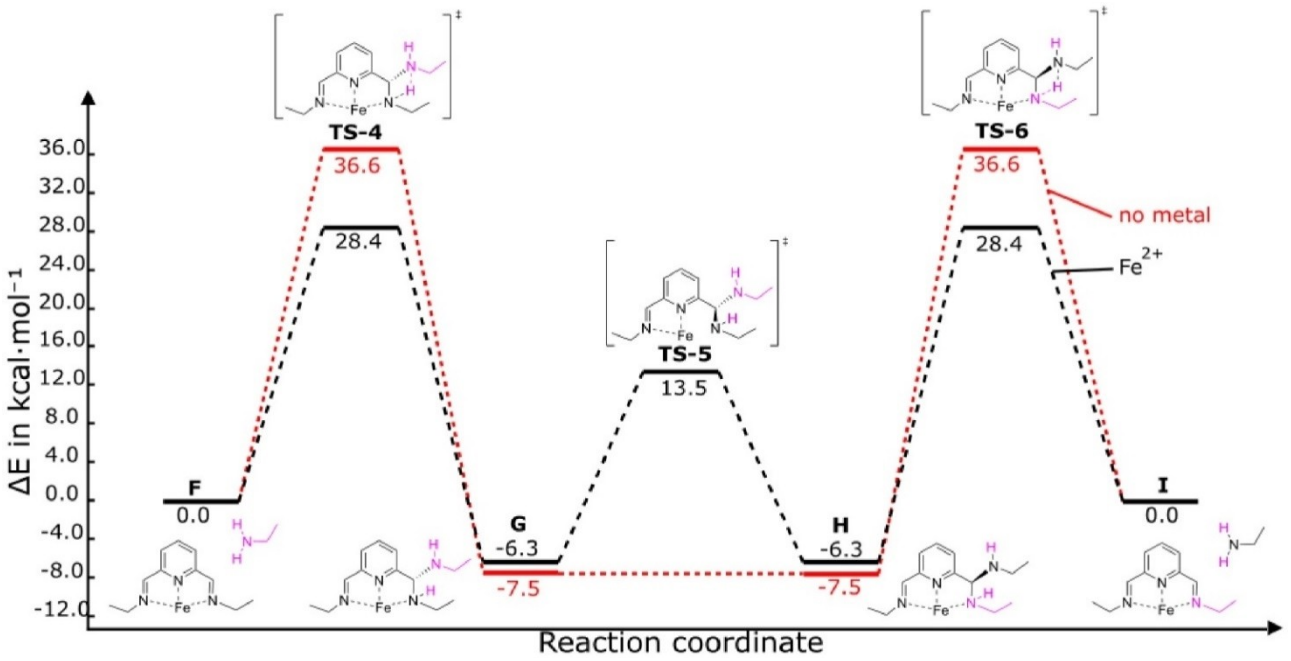

Figure 4. Energy profile for the transimination reaction between [iron(II) 2,6-bis-ethylimine pyridine $(NCCH_3)_3]^{2+}$ and ethylamine (black), and between 2,6-bis-ethylimine pyridine and ethylamine (red), calculated without explicit solvation. The second proton transfer, from **H** to **TS-6**, is rate-limiting with an energy barrier of 34.7 and 44.1 kcal/mol, respectively. Structures of the black pathway are provided. For clarification, the incoming ethylamine has been colored pink.

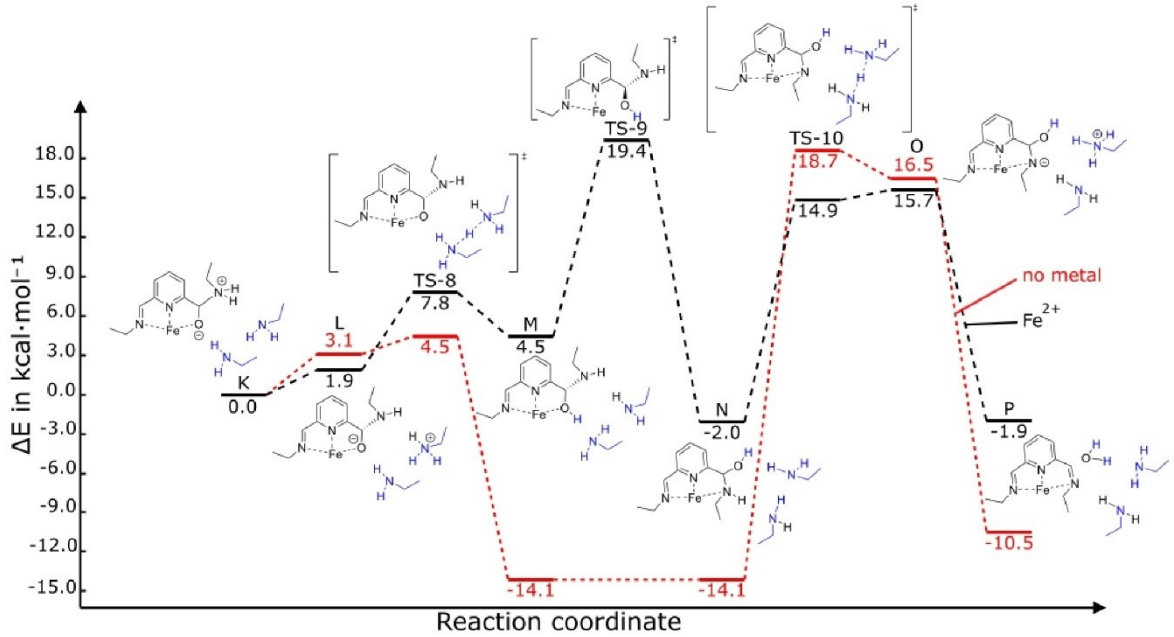

Figure 5. Gibbs free energy profile for the condensation reaction between ethylamine and [iron(II) 2-methoxo-6-ethylimine pyridine $(NCCH_3)_3]^{2+}$ (black), and 2-methoxo-6-ethylimine pyridine (red), both with two additional ethylamines acting as proton shuttles, calculated without explicit solvation. At 19.4 kcal/mol, the rotation **TS-9** is rate-limiting if Fe^{2+} is present. In absence of a metal, the barrier of 32.8 kcal/mol from **N** to **TS-10** is rate-limiting. Structures of the black pathway are provided. For clarification, the mediating ethylamines have been colored blue.

Condensation Reaction With Proton-Shuttling Amines

To bypass the high-energy barriers resulting from the 4-membered ring TS route, we investigated proton transfers facilitated by proton shuttles, as is known to work in experimental setting[74–76] and has been calculated recently for metal-free dynamic exchanges.[64–65,77] According to Rufino and Pliego,[65] using two water molecules as shuttle decreases the energy barrier for condensation of acetaldehyde with methylamine from 47.7 to 26.4 kcal/mol (in toluene at 298 K). Using a carboxylic acid group as proton shuttle further reduces the barrier to 15.8 kcal/mol (in acetonitrile or toluene, at 298 K).

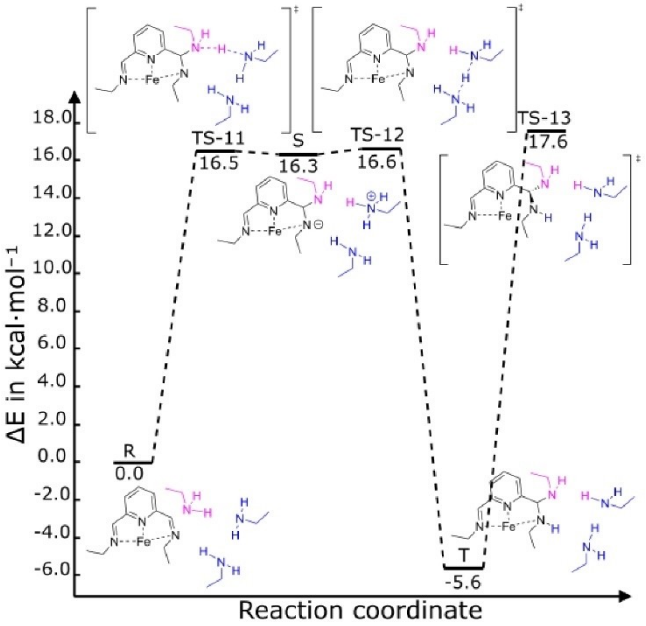

Figure 6. Energy profile for the mediated transimination reaction between [iron(II) 2,6-bis-ethylimine pyridine $(NCCH_3)_3]^{2+}$ and ethylamine, calculated without explicit solvation. With 23.3 kcal/mol, rotation of the aminal (**T** to **TS-13**) is rate-limiting. For clarification, the incoming ethylamine has been colored pink and the mediating ethylamines are blue.

Kirmizialtin and co-workers[77] have shown that the calculated cost of condensation of oximes in water can be reduced from 31.4 kcal/mol to 12.9 kcal/mol by adding two explicit water molecules. These promising studies enticed us to investigate the role of proton shuttles for the hitherto not-studied case of metal-stabilized pincer molecules. This is especially relevant since here not only the TS might be stabilized by proton shuttles, but the starting materials, of course, also by metal ions (and, for example, inverting the equilibrium between aldehydes and imines from 'towards aldehydes' without metal coordination to 'towards imines' with metal coordination).[78] In the dynamic polymer systems that form the experimental basis for our calculations,[52] only trace amounts of water are present, whereas free amines are present in excess. Therefore, two ethylamines were used as proton shuttles in the calculation of the condensation reaction between [iron(II) 2-methoxo-6-ethylimine pyridine $(NCCH_3)_3]^{2+}$ and ethylamine (Figure 5, in black). The two hydrogen transfers (turning R–NH_2 into R–N=C) were thereby transformed to multistep processes involving eight-membered rings.

Starting from adduct **K**, a proton was transferred from the incoming ethylamine to the first mediating ethylamine, leading to intermediate **L** (+1.9 kcal/mol). Then, another proton on that ethyl amine is moved from the first to the second mediating ethylamine, requiring another 5.9 kcal/mol (transition state **TS-8**). Finally, a similar, third proton movement from the second mediating ethylamine to the aldehyde on the pincer completed the first transfer into hemiaminal **M**. Various scans and IRC calculations have shown that there is no intermediate between transition state **TS-8** and hemiaminal **M**. Rotation of the hemiaminal from one coordination to the other, thus from **M** to **N**, required an additional 14.9 kcal/mol. The proton-shuttling amines are not involved in this step. This rotation **TS-9** is rate-determining with $\Delta G^{\ddagger}$ 19.4 kcal/mol.

The second mediated proton transfer followed an analogous path, but now the proton moves backwards. Starting at hemiaminal **N**, a proton is moved from the donating ethylimine to the first mediating ethylamine, followed immediately by a second proton transfer from the first mediating ethylamine to the second. This transition state **TS-10** required 16.9 kcal/mol, and only showed the movement of the second proton; multiple scans and IRCs did not yield a stable intermediate with an ammonium-like structure for the bottom amine molecule (see molecular structures in Figure 5) between hemiaminal **N** and **TS-10**. After **TS-10**, we found stable intermediate **O** at 15.7 kcal/mol, in which the top ethylamine had the extra proton. A final proton transfer lead to water elimination, resulting in the product **P** at −1.9 kcal/mol. Compared to the non-mediated pathway, the gain is significant, reducing the energy barrier from more than 50 kcal/mol to just 19.4 kcal/mol. The ethylamine-mediated route can thus be considered a viable reaction at room temperature.

This mediated condensation reaction was also calculated in the absence of a metal center (Figure 5, in red). The first proton transfer now required less energy in the absence of Fe^{2+}, and the hemiaminal **M** without metal center was very stable (−14.1 kcal/mol), much more than the Fe^{2+}-coordinated hemiaminal **M** (4.5 kcal/mol). Although the energies of **TS-10** of both systems were in the same range, the energy barrier for condensation without metal was much larger (32.8 kcal/mol), due to the higher stability of the hemiaminal **N**. Imine pincer **P** is more stable as well (−10.5 kcal/mol instead of −1.9 kcal/mol).

As a consequence, backwards reaction from imine pincer **P** to adduct **K** has an energy barrier of 29.2 kcal/mol in its first two proton transfers, with hemiaminal **M** as most stable structure.

In this amine-mediated condensation reaction, we have thus again shown the catalyzing effect of Fe^{2+}-coordination. It lowers the energy barrier from 32.8 kcal/mol to 19.4 kcal/mol, and provides the driving force to push the condensation from hemiaminal to pincer complex to completion.

Transimination Reaction With Proton-Shuttling Amines

Subsequently, the transimination reaction was also calculated for [iron(II) 2,6-bis-ethylimine pyridine $(NCCH_3)_3]^{2+}$ and ethylamine with two extra ethylamines acting as proton shuttles. As the transimination reaction is symmetrical, the reaction is only calculated until the rotation of the aminal (Figure 6).

The amine-mediated proton transfer yields two transition states **TS-11** and **TS-12** and an intermediate **S**, all around 16.5 kcal/mol. The formed aminal **T** was found at −5.6 kcal/mol compared to the starting materials, and the rotation of the aminal **TS-13** at 17.6 kcal/mol. Analogously to the condensation reaction, the proton-shuttling lowered the activation energy of the proton transfer to such an extent that the rotation is now

rate-determining. With a total energy barrier of 23.2 kcal/mol, we can conclude that this mediated transimination reaction is plausible at room temperature.

Condensation Reaction With Two Pincer ligands

In all calculations, we have – for reasons of computational efficiency – assumed coordination of a single pincer and three acetonitrile molecules to the metal center. However, we know from experimental work that double pincers (i.e., the pincers exist as 1:2 metal/ligand complex) are predominant.[52] To validate the computational approach taken, we also performed the calculation of the condensation reaction of Fe^{2+} with two pincer ligands (Supporting Information section S4). This reaction displayed an energy path similar to the one with a single pincer and three acetonitrile ligands, with only slightly higher energy barriers for the proton transfers via the four-membered ring TS. Following this result, we considered our use of single pincer complexes as a valid computational simplification.

Varying the Amine-Based Nucleophile and Substituents in the Non-Amine-Mediated Condensation Reaction

The exchange reactions under current study can be readily varied using different nucleophiles and changing various electronic factors of possible importance, as has indeed been done experimentally to quite some detail.[28,52,79–80] We have thus compared the condensation reactions of the aldehyde pincer with ethylamine, methylhydrazine or methoxyamine as nucleophiles (Supporting Information section S5). As we have taken the four-membered ring transition state for proton transfer, $\Delta G^{\ddagger}$ remains high ($>$ 47.8 kcal/mol).

In non-coordinated aromatic imines, substituents on the ring have strong influence on the reactivity of the imine, as they alter the electron density of the imine.[39] In the presence of a metal, this could be different. The condensation reaction was therefore calculated for pincers in which the X and Y positions were altered (Figure 1, Supporting Information section S6). Substitution of the hydrogen atom on the X-position by the electron-withdrawing $-CF_3$ group or the electron-donating $-OCH_3$ group resulted in less than 2 kcal/mol change in any step, regardless of the nature of the imine and amine of the system. Additionally, when changing the non-reactive imine of a double pincer from ethylimine to hydrazone or methoxime (position Y in Figure 1), no changes in energy were observed either (Table S2). Substitutions of the R', X and Y positions in the transimination reaction showed similar results (Supporting Information sections S7 and S8) We can therefore conclude that neither meta-position is relevant to our imine exchanges. Neither factor is expected to change in character when considering the amine-mediated reactions, suggesting that rotation of the (hemi)aminal is indeed the energetically most relevant process.

Conclusions

We studied the condensation reaction of a metal-coordinated aldehyde pincer with ethylamine, via either a four-membered ring transition state (TS) for the proton transfers, as previously proposed in the literature, or via an unstrained TS involving two proton shuttles. The former activation barrier was calculated to be much higher (52 kcal/mol) than experimentally observed (the reaction proceeds readily at room temperature), making such a strained TS unlikely. In contrast, with the involvement of two ethyl amines as proton shuttles the calculated activation energy dropped to 19 kcal/mol, which is compatible with experiments. This confirmed our hypothesis that the imposed ring strain of the four-membered transition state unnecessarily increased the energy barrier. While this insight was previously known for single proton shuttles,[65] here we demonstrated its viability in acetonitrile with multiple amines in the presence of a metal center.

For the transimination reaction a similar reduction in activation energy was found: the non-mediated pathways required 34–43 kcal/mol depending on the nature of studied amine, whereas the amine-mediated proton transfer required only 23 kcal/mol. These calculations thus explain the advantages of the experimentally common addition of a small excess of free amine in the production of dynamic imine/amine-based vitrimer materials to speed up the exchange.[81–82]

Titration experiments showed that Fe^{2+} binds stronger to the studied pincers than Zn^{2+}. Calculation of the condensation reaction without proton shuttles further confirmed that the Fe^{2+} is better suited for these imine exchange reactions. Finally, our calculations also provide – for the first time – theoretical support for the stabilizing effect of coordination of the imine to the metal center, which was already experimentally found in cage formations[43] and other subcomponent self-assemblies.[51]

Experimental Section

Computational Methods

Density functional calculations (DFT) – geometry optimization, vibrational frequency calculations and IRC calculations – were performed using the Gaussian 16 suite of programs,[83] with the wB97XD functional[84–85] and 6-311G(2d,2p) basis set as implemented in there. Although transition metals such as iron are well-defined in this basis set, geometry connectivity was added to ensure coordination to the iron where desired. All (natural population) charges and Wiberg bond orders were calculated using the NBO 3.1 program as implemented in Gaussian 16. Generic solvent effects were incorporated by using the universal solvation model based on density (SMD).[86] Acetonitrile was chosen as the model solvent, as experimental work on imine pincer-based polymers has been reported for acetonitrile.[52] Gibbs free energies are reported in a standard state: at 298 K and 1 bar pressure. Output of all geometry optimizations is provided in the Supporting Information (sections S9 and S10).

In each reaction step in which more than one molecule is involved (e.g., structures **A** and **E** in Figure 3), all molecules were calculated as part of a single computation at a minimum 3.6 Å distance. In the

mediated pathways however, all starting and ending molecules were calculated separately. For crucial transition states, full IRC analysis was performed, confirming the nature of the transition state. The rotational transition state of the transimination reaction (**TS-2** in Figure 3) required multiple extensive rotational scans, followed by a transition state search involving IOp(1/8 = 2). For computational simplicity, only a single pincer was coordinated to an iron(II) center. The other three coordination sites were occupied by explicit acetonitrile ligands (Figure 1).

Materials and Methods

^{1}H NMR and ^{13}C NMR spectra were recorded on a Bruker Avance III 400 spectrometer (observation of ^{1}H nucleus at 400 MHz, and of ^{13}C nucleus at 101 MHz). Chemical shifts are reported in parts per million (ppm), calibrated on the residual peak of the solvent, whose values are referred to tetramethylsilane (TMS, $\delta_{TMS} = 0$ ppm), as the internal standard. ^{13}C NMR spectra were performed with proton decoupling. High-resolution ESI mass spectra were recorded on a Thermo Scientific Q Exactive High-Resolution mass spectrometer. UV-vis spectra were recorded on a Varian Cary 50 spectrophotometer.

Synthesis of the diiminepyridine pincer: 2,6-pyridinedicarboxaldehyde (5.2 mmol, 700 mg) was dissolved in 35 mL absolute methanol, containing molecular sieves. Aniline (10.4 mmol, 975 μL) was added to the solution and the reaction mixture was stirred under reflux for 2 h. The hot reaction mixture was filtered, over a normal filter and washed with hot methanol (50 °C). The solvent was removed in vacuo. The product was dried in the oven overnight and obtained as yellowish powder in 1.22 g yield (82 %). ^{1}H NMR (400 MHz, Chloroform-d) δ 8.70 (s, 2H), 8.31 (d, J = 7.8 Hz, 2H), 7.96 (t, J = 7.8 Hz, 1H), 7.44 (dd, J = 8.4, 7.2 Hz, 4H), 7.36–7.28 (m, 6H). ^{13}C NMR (101 MHz, Chloroform-d) δ 160.14, 154.66, 150.84, 137.30, 129.26, 129.25, 126.90, 123.23, 123.19, 121.18, 121.16, 77.21. High-res. MS (ESI): Expected for $[M+H]^+$ 286.1339, found 286.1339.

Titration: For the metal-to-ligand titration two solutions were prepared. A: ligand (i.e., diiminepyridine) solution (without metal salt) in acetonitrile ($1.0 \cdot 10^{-5}$ M), and B: ligand solution with 5 equivalent of metal salt in acetonitrile. Ligand concentration was $1.0 \cdot 10^{-5}$ M, while metal concentration was $5.0 \cdot 10^{-5}$ M. As metal salt, $Fe(Otf)_2$ and $Zn(Otf)_2$ were used.

Mixing solutions A and B in the appropriate ratio allowed for the titration curve of each metal to be recorded by UV-vis spectrometry. After mixing, 30 min of equilibration time was allowed. Figure 2a shows the UV-vis spectra of the ligand without metal, and with either Fe^{2+} or Zn^{2+}. Figure 2b show the (normalized) absorption as function of equivalence of metal added (recorded at 613 nm for Fe^{2+} and at 370 nm at Zn^{2+}).

Supporting Information

The authors have cited additional references within the Supporting Information (Ref. [87–88]).

Acknowledgements

This research was conducted under project number S62.3.15577 in the framework of the Partnership Program of the Materials innovation institute M2i (www.m2i.nl) and the Technology Foundation TTW (www.stw.nl), which is part of the Dutch Research Council (www.nwo.nl). Shanice Veraar is kindly thanked for her help with the experimental work. Dr. Guanna Li, Dr. Sybren Schoustra and Simon van Hurne are acknowledged for fruitful discussions.

Conflict of Interests

The authors declare no conflict of interest.

Data Availability Statement

The data that support the findings of this study are available from the corresponding author upon reasonable request.

Keywords: DFT calculations · imines · pincer compounds · proton shuttle

[1] S. J. Rowan, S. J. Cantrill, G. R. L. Cousins, J. K. M. Sanders, J. F. Stoddart, *Angew. Chem. Int. Ed.* **2002**, *41*, 898.
[2] *Dynamic Covalent Chemistry: Principles, Reactions, and Applications* (Eds: W. Zhang, Y. Jin), John Wiley & Sons Ltd., Chichester, UK, **2017**.
[3] A. Herrmann, *Chem. Soc. Rev.* **2014**, *43*, 1899.
[4] F. García, M. M. J. Smulders, *J. Polym. Sci. Part A* **2016**, *54*, 3551.
[5] J. W. Sadownik, R. V. Ulijn, *Curr. Opin. Biotechnol.* **2010**, *21*, 401.
[6] N. Zheng, Y. Xu, Q. Zhao, T. Xie, *Chem. Rev.* **2021**, *121*, 1716.
[7] M. Mondal, A. K. H. Hirsch, *Chem. Soc. Rev.* **2015**, *44*, 2455.
[8] Y. Chao, A. Krishna, M. Subramaniam, D.-D. Liang, S. P. Pujari, A. C.-H. Sue, G. Li, F. M. Miloserdov, H. Zuilhof, *Angew. Chem. Int. Ed.* **2022**, *61*, e202207456.
[9] C. J. Kloxin, C. N. Bowman, *Chem. Soc. Rev.* **2013**, *42*, 7161.
[10] M. Podgórski, B. D. Fairbanks, B. E. Kirkpatrick, M. McBride, A. Martinez, A. Dobson, N. J. Bongiardina, C. N. Bowman, *Adv. Mater.* **2020**, *32*, 2070158.
[11] N. J. Van Zee, R. Nicolaÿ, *Prog. Polym. Sci.* **2020**, 101233.
[12] G. M. Scheutz, J. J. Lessard, M. B. Sims, B. S. Sumerlin, *J. Am. Chem. Soc.* **2019**, *41*, 16181.
[13] M. Guerre, C. Taplan, J. M. Winne, F. E. Du Prez, *Chem. Sci.* **2020**, *11*, 4855.
[14] P. Chakma, D. Konkolewicz, *Angew. Chem. Int. Ed.* **2019**, *58*, 9682.
[15] J. Zheng, Z. M. Png, S. H. Ng, G. X. Tham, E. Ye, S. S. Goh, X. J. Loh, Z. Li, *Mater. Today* **2021**.
[16] K. R. West, K. D. Bake, S. Otto, *Org. Lett.* **2005**, *7*, 2615.
[17] S. M. Elbert, N. I. Regenauer, D. Schindler, W.-S. Zhang, F. Rominger, R. R. Schröder, M. Mastalerz, *Chem. Eur. J.* **2018**, *24*, 11438.
[18] K. Acharyya, P. S. Mukherjee, *Angew. Chem. Int. Ed.* **2019**, *58*, 8640.
[19] A. J. McConnell, *Chem. Soc. Rev.* **2022**, *51*, 2957.
[20] E. N. Keyzer, A. Sava, T. K. Ronson, J. R. Nitschke, A. J. McConnell, *Chem. Eur. J.* **2018**, *24*, 12000.
[21] D. Zhang, T. K. Ronson, J. R. Nitschke, *Acc. Chem. Res.* **2018**, *51*, 2423.
[22] Y. Fang, J. A. Powell, E. Li, Q. Wang, Z. Perry, A. Kirchon, X. Yang, Z. Xiao, C. Zhu, L. Zhang, F. Huang, H.-C. Zhou, *Chem. Soc. Rev.* **2019**, *48*, 4707.
[23] M. von Delius, E. M. Geertsema, D. A. Leigh, *Nat. Chem.* **2010**, *2*, 96.
[24] J. Hu, S. K. Gupta, J. Ozdemir, M. H. Beyzavi, *ACS Appl. Nano Mater.* **2020**, *3*, 6239.
[25] M. E. Belowich, J. F. Stoddart, *Chem. Soc. Rev.* **2012**, *41*, 2003.
[26] E. H. Cordes, W. P. Jencks, *J. Am. Chem. Soc.* **1962**, *84*, 826.
[27] M. Ciaccia, S. Di Stefano, *Org. Biomol. Chem.* **2015**, *13*, 646.
[28] P. Kovaříček, J.-M. Lehn, *J. Am. Chem. Soc.* **2012**, *134*, 9446.
[29] J. C. Lauer, W.-S. Zhang, F. Rominger, R. R. Schröder, M. Mastalerz, *Chem. Eur. J.* **2018**, *24*, 1816.
[30] B. P. Benke, T. Kirschbaum, J. Graf, J. H. Gross, M. Mastalerz, *Nat. Chem.* **2023**, *15*, 413.
[31] O. Storm, U. Lüning, *Chem. Eur. J.* **2002**, *8*, 793.
[32] K. Ziach, J. Jurczak, *Org. Lett.* **2008**, *10*, 5159.
[33] N. Giuseppone, J.-L. Schmitt, J.-M. Lehn, *Angew. Chem. Int. Ed.* **2004**, *43*, 4902.

[34] N. Giuseppone, J.-L. Schmitt, J.-M. Lehn, *J. Am. Chem. Soc.* **2006**, *128*, 16748.
[35] P. Pandey, A. P. Katsoulidis, I. Eryazici, Y. Wu, M. G. Kanatzidis, S. T. Nguyen, *Chem. Mater.* **2010**, *22*, 4974.
[36] A. Natraj, W. Ji, J. Xin, I. Castano, D. W. Burke, A. M. Evans, M. J. Strauss, M. Ateia, L. S. Hamachi, N. C. Gianneschi, Z. A. Alothman, J. Sun, K. Yusuf, W. R. Dichtel, *J. Am. Chem. Soc.* **2022**, *144*, 19813.
[37] F. J. Uribe-Romo, J. R. Hunt, H. Furukawa, C. Klöck, M. O'Keeffe, O. M. Yaghi, *J. Am. Chem. Soc.* **2009**, *131*, 4570.
[38] E. Dautzenberg, M. Lam, G. Li, L. C. P. M. de Smet, *Nanoscale* **2021**, *13*, 19446.
[39] S. K. Schoustra, J. A. Dijksman, H. Zuilhof, M. M. J. Smulders, *Chem. Sci.* **2021**, *12*, 293.
[40] C. Godoy-Alcántar, A. K. Yatsimirsky, J. M. Lehn, *J. Phys. Org. Chem.* **2005**, *18*, 979.
[41] P. Mal, D. Schultz, K. Beyeh, K. Rissanen, J. R. Nitschke, *Angew. Chem. Int. Ed.* **2008**, *47*, 8297.
[42] J. R. Nitschke, J.-M. Lehn, *Proc. Natl. Acad. Sci. USA* **2003**, *100*, 11970.
[43] D.-H. Ren, D. Qiu, C.-Y. Pang, Z. Li, Z.-G. Gu, *Chem. Commun.* **2015**, *51*, 788.
[44] J. R. Nitschke, *Acc. Chem. Res.* **2007**, *40*, 103.
[45] D. Schultz, J. R. Nitschke, *J. Am. Chem. Soc.* **2006**, *128*, 9887.
[46] J. Anhäuser, R. Puttreddy, L. Glanz, A. Schneider, M. Engeser, K. Rissanen, A. Lützen, *Chem. Eur. J.* **2019**, *25*, 12294.
[47] J. I. van der Vlugt, S. Demeshko, S. Dechert, F. Meyer, *Inorg. Chem.* **2008**, *47*, 1576.
[48] T. J. Burchell, R. J. Puddephatt, *Inorg. Chem.* **2005**, *44*, 3718.
[49] H. Bunzen, Nonappa, E. Kalenius, S. Hietala, E. Kolehmainen, *Chem. Eur. J.* **2013**, *19*, 12978.
[50] C. D. Meyer, C. S. Joiner, J. F. Stoddart, *Chem. Soc. Rev.* **2007**, *36*, 1705.
[51] S. Kitagawa, R. Kitaura, S.-i. Noro, *Angew. Chem. Int. Ed.* **2004**, *43*, 2334.
[52] F. García, J. Pelss, H. Zuilhof, M. M. J. Smulders, *Chem. Commun.* **2016**, *52*, 9059.
[53] P. E. Figgins, D. H. Busch, *J. Am. Chem. Soc.* **1960**, *82*, 820.
[54] R. Lavendomme, T. K. Ronson, J. R. Nitschke, *J. Am. Chem. Soc.* **2019**, *141*, 12147.
[55] C. D. Pentecost, K. S. Chichak, A. J. Peters, G. W. V. Cave, S. J. Cantrill, J. F. Stoddart, *Angew. Chem. Int. Ed.* **2007**, *46*, 218.
[56] G. Nasr, T. Macron, A. Gilles, Z. Mouline, M. Barboiu, *Chem. Commun.* **2012**, *48*, 6827.
[57] D.-P. Wang, J.-C. Lai, H.-Y. Lai, S.-R. Mo, K.-Y. Zeng, C.-H. Li, J.-L. Zuo, *Inorg. Chem.* **2018**, *57*, 3232.
[58] Y. Zhang, M. Barboiu, *ChemistryOpen* **2019**, *8*, 1345.
[59] I. Kocsis, D. Dumitrescu, Y.-M. Legrand, A. van der Lee, I. Grosu, M. Barboiu, *Chem. Commun.* **2014**, *50*, 2621.
[60] L. Hogg, D. A. Leigh, P. J. Lusby, A. Morelli, S. Parsons, J. K. Y. Wong, *Angew. Chem. Int. Ed.* **2004**, *43*, 1218.
[61] D. A. Leigh, P. J. Lusby, S. J. Teat, A. J. Wilson, J. K. Y. Wong, *Angew. Chem. Int. Ed.* **2001**, *40*, 1538.
[62] C. Browne, T. K. Ronson, J. R. Nitschke, *Angew. Chem. Int. Ed.* **2014**, *53*, 10701.
[63] M. Ciaccia, R. Cacciapaglia, P. Mencarelli, L. Mandolini, S. Di Stefano, *Chem. Sci.* **2013**, *4*, 2253.
[64] R. Pérez-Soto, M. Besora, F. Maseras, *Org. Lett.* **2020**, *22*, 2873.
[65] V. C. Rufino, J. R. Pliego, *Comput. Theor. Chem.* **2020**, *1191*, 113053.
[66] H. Zheng, H. Ye, X. Yu, L. You, *J. Am. Chem. Soc.* **2019**, *141*, 8825.
[67] G. Olivo, O. Lanzalunga, S. Di Stefano, *Adv. Synth. Catal.* **2016**, *358*, 843.
[68] S. K. Schoustra, M. M. J. Smulders, *Macromol. Rapid Commun.* **2023**, *44*, 2200790.
[69] C. Fonseca Guerra, P. J. Sanz Miguel, A. Cebollada, F. M. Bickelhaupt, B. Lippert, *Chem. Eur. J.* **2014**, *20*, 9494.
[70] R. H. Holyer, C. D. Hubbard, S. F. A. Kettle, R. G. Wilkins, *Inorg. Chem.* **1966**, *5*, 622.
[71] R. A. Angnes, *GitHub repository* **2020**, DOI 10.5281/zenodo.4065333.
[72] L. Shen, N. Cao, L. Tong, X. Zhang, G. Wu, T. Jiao, Q. Yin, J. Zhu, Y. Pan, H. Li, *Angew. Chem. Int. Ed.* **2018**, *57*, 16486.
[73] T. Jiao, G. Wu, Y. Zhang, L. Shen, Y. Lei, C.-Y. Wang, A. C. Fahrenbach, H. Li, *Angew. Chem. Int. Ed.* **2020**, *59*, 18350.
[74] F. Schaufelberger, K. Seigel, O. Ramström, *Chem. Eur. J.* **2020**, *26*, 15581.
[75] A. Dirksen, T. M. Hackeng, P. E. Dawson, *Angew. Chem. Int. Ed.* **2006**, *45*, 7581.
[76] N. Wilhelms, S. Kulchat, J.-M. Lehn, *Helv. Chim. Acta* **2012**, *95*, 2635.
[77] S. Kirmizialtin, B. S. Yildiz, I. Yildiz, *J. Phys. Org. Chem.* **2017**, *30*, e3711.
[78] D. Schultz, J. R. Nitschke, *Angew. Chem. Int. Ed.* **2006**, *45*, 2453.
[79] F. Schaufelberger, O. Ramström, *J. Am. Chem. Soc.* **2016**, *138*, 7836.
[80] Y. R. Hristova, M. M. J. Smulders, J. K. Clegg, B. Breiner, J. R. Nitschke, *Chem. Sci.* **2011**, *2*, 638.
[81] A. Liguori, M. Hakkarainen, *Macromol. Rapid Commun.* **2022**, *43*, 2100816.
[82] F. Van Lijsebetten, K. De Bruycker, Y. Spiesschaert, J. M. Winne, F. E. Du Prez, *Angew. Chem. Int. Ed.* **2022**, *61*, e202113872.
[83] M. J. Frisch, G. W. Trucks, H. B. Schlegel, G. E. Scuseria, M. A. Robb, J. R. Cheeseman, G. Scalmani, V. Barone, G. A. Petersson, H. Nakatsuji, X. Li, M. Caricato, A. V. Marenich, J. Bloino, B. G. Janesko, R. Gomperts, B. Mennucci, H. P. Hratchian, J. V. Ortiz, A. F. Izmaylov, J. L. Sonnenberg, Williams, F. Ding, F. Lipparini, F. Egidi, J. Goings, B. Peng, A. Petrone, T. Henderson, D. Ranasinghe, V. G. Zakrzewski, J. Gao, N. Rega, G. Zheng, W. Liang, M. Hada, M. Ehara, K. Toyota, R. Fukuda, J. Hasegawa, M. Ishida, T. Nakajima, Y. Honda, O. Kitao, H. Nakai, T. Vreven, K. Throssell, J. A. Montgomery Jr., J. E. Peralta, F. Ogliaro, M. J. Bearpark, J. J. Heyd, E. N. Brothers, K. N. Kudin, V. N. Staroverov, T. A. Keith, R. Kobayashi, J. Normand, K. Raghavachari, A. P. Rendell, J. C. Burant, S. S. Iyengar, J. Tomasi, M. Cossi, J. M. Millam, M. Klene, C. Adamo, R. Cammi, J. W. Ochterski, R. L. Martin, K. Morokuma, O. Farkas, J. B. Foresman, D. J. Fox, *Gaussian 16 Rev. C.01*, Wallingford, CT, **2016**.
[84] J.-D. Chai, M. Head-Gordon, *Phys. Chem. Chem. Phys.* **2008**, *10*, 6615.
[85] Y. Minenkov, Å. Singstad, G. Occhipinti, V. R. Jensen, *Dalton Trans.* **2012**, *41*, 5526.
[86] A. V. Marenich, C. J. Cramer, D. G. Truhlar, *J. Phys. Chem. B* **2009**, *113*, 6378.
[87] S. Kulchat, M. N. Chaur, J.-M. Lehn, *Chem. Eur. J.* **2017**, *23*, 11108.
[88] M. He, J.-M. Lehn, *J. Am. Chem. Soc.* **2019**, *141*, 18560.

Manuscript received: June 5, 2023
Accepted manuscript online: August 10, 2023
Version of record online: ■■, ■■

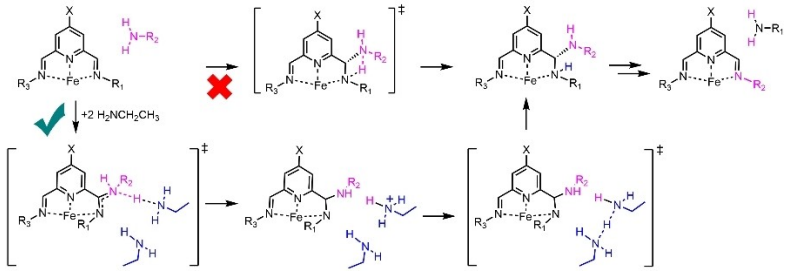

A. van Dam, R. van Schendel, Dr. S. Gangarapu, Prof. H. Zuilhof, Dr. M. M. J. Smulders**

1 – 10

DFT Study of Imine-Exchange Reactions in Iron(II)-Coordinated Pincers

Proton shuttle: A DFT study on condensation and transimination reactions of an Fe^{2+}-coordinated diimine pyridine pincer was conducted. Titration experiments confirmed the use of Fe^{2+} as a model metal ion, after which the reactions were investigated computationally using traditional four-membered ring transition states for proton transfer. When those displayed unrealistic high energy barriers, two ethylamines were added to function as proton shuttles, which lowered the activation energies to realistic values.